Flat-band engineering of quasi-one-dimensional systems via supersymmetric transformations

V. Jakubský [1] and K. Zelaya [2]

[1]*Nuclear Physics Institute, Czech Academy of Science*, 250 68 Řež, Czech Republic
[2]*Department of Physics, Queens College of the City University of New York*, Queens, New York 11367, USA

We introduce a systematic method to spectrally design quasi-one-dimensional crystal models described by the Dirac equation in the low-energy regime. The method is based on the supersymmetric transformation applied to an initially known pseudo-spin-1/2 model. This allows one to extend the corresponding supersymmetric partner so that the new model describes a pseudo-spin-1 system. The spectral design allows the introduction of a flat band and discrete energies at will into the new model. The results are illustrated in three examples where the Su-Schriefer-Heeger chain is locally converted into a stub lattice.

I. INTRODUCTION

Recent developments in experimental techniques have facilitated the creation of artificial materials through molecular manipulations [1–5], photonic lattices [6,7], and phononic experiments [8,9]. The latter provide unprecedented control over physical properties and effective interactions in the created systems. Particularly, it is possible to prepare one-dimensional crystallic chains with diverse structure, e.g., Su-Schriefer-Heeger, stub, diamond (rhombic), Creutz, or fishbone lattices [7,10,11]. These systems attract attention due to their simple structure yet rich properties, e.g., existence of topological states [12–15], bulk-edge correspondence [16], Aharonov-Bohm caging [17–20], and superconductivity [21,22]. Many of these properties are related to the existence of a flat band in their spectra. The flat band is associated with vanishing group velocity and macroscopical degeneration of eigenstates. It was observed experimentally in optical lattices [11,23–25].

Both experimental [10] and theoretical [26,27] efforts have been made to provide useful tools and methods for engineering flat-band systems. For instance, via repetition of microarrays [26], utilizing polynomials of a tight-binding Hamiltonian [27], through compact localized states classification [28], and using graph theory [29,30]. The latter frequently rely on the tight-binding approach. In this article, we resolve to the Dirac approximation valid for low-energy systems, where the dynamics is described by the Dirac equation with pseudospin one. Our approach is based on supersymmetric quantum mechanics so that the existence of a flat band is granted by construction.

Supersymmetric (susy) transformations, equivalently known in the literature as Darboux transformations, are specific nonunitary mappings between evolution equations of two quantum systems. The latter can be used for the construction of the new solvable models, where the potential term of the initial system gets deformed, yet the knowledge of the solutions is preserved. These transformations have been broadly explored in nonrelativistic quantum mechanics [31] and, in recent years, in the construction of solvable models described by one- or two-dimensional Dirac equations. Supersymmetric transformations for low-dimensional Dirac operators was discussed in [32,33] and employed in a series of works; see, e.g., [34–44]. Most of these works focus on the analysis of pseudo-spin-1/2 quantum systems, but it was recently applied in the context of pseudo-spin-1 flat-band systems in [45].

The Su-Schriefer-Heeger (SSH) model is a one-dimensional chain of dimerized atoms, used originally for the analysis of solitonic effects in macromolecules [46,47] and known for possessing nontrivial topological properties [48]. The low-energy approximation of its tight-binding Hamiltonian corresponds to the one-dimensional Dirac operator [47]. Interestingly, solitonic states emerge in SSH ladders on domain walls, where the dimerization of atoms gets inverted. Domain walls on SSH-type chains of coupled dimers were experimentally realized on chlorine vacancies in the c(2 × 2) adsorption layer on Cu(100) in [13]. The existence of topological domain-wall states was discussed in [49,50], whereas the supersymmetric transformation has been applied to induce a topological gapped state in the SSH chain [51,52]. Furthermore, the transmission properties of pseudo-spin-1 Dirac equations described through decorated, "bearded," SSH chains have been discussed [53]. The spectral and symmetry properties of a trimer SSH chain with next-nearest interaction were considered in [54].

In this article, the supersymmetric transformation is exploited to connect known pseudo-spin-1/2 quantum models with new unknown pseudo-spin-1 models. Particularly, the transformation allows one to tune the emerging flat band of the new model, while adding new bound state energies, assuming that the proper boundary conditions are met. To this end, a pseudo-spin-1/2 model is trivially extended into a pseudo-spin-1 system by adding an isolated coupling term,
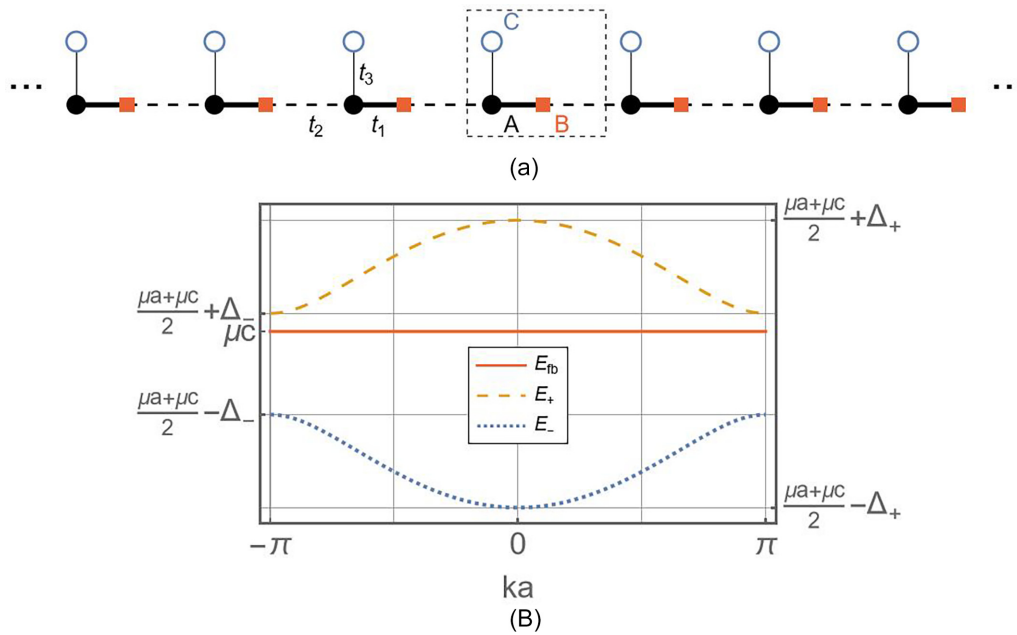
FIG. 1. (a) Sketch of the periodic pseudo-one-dimensional stub lattice with three atoms A, B, and C per unitary cell (dashed rectangle). The hopping parameters are denoted by t_1, t_2, and t_3. (b) Dispersion relations (5) in terms of the hopping parameters and the on-site interactions μ_A and $\mu_B = \mu_C$, where $\Delta_\pm = \sqrt{(t_1 \pm t_2)^2 + t_3^2 + \frac{(\mu_A - \mu_C)^2}{4}}$.

such that the dispersion relations are kept invariant. The supersymmetric transformation of such an energy operator is then matched with a new and nontrivially extended pseudo-spin-1 Hamiltonian, where the added coupled term is no longer isolated and now describes an interaction with the rest of the elements in the system. Particularly, a graphenelike system is used as the initial model in the transformation, leading to explicit models that behave asymptotically as an SSH chain with altered dimerization patterns resembling the domain wall. Such an SSH chain gets locally decorated by additional atoms, forming a stub lattice in the localized region. This allows for a systematic mechanism to spectrally manufacture pseudo-spin-1 models based on relatively simple pseudo-spin-1/2 counterparts.

The manuscript is structured as follows. Section II summarizes the periodic structure and dispersion bands of the generalized stub lattice, where the special case where a flat band emerges is considered. In Sec. III, the general framework of the Darboux transform for arbitrary pseudospin systems is briefly introduced. Here, the transformation is implemented for an extended pseudo-spin-1/2 so that the susy partner renders a nontrivial pseudo-spin-1 model. Applications of the latter are further exemplified in Secs. IV and V, where explicit cases of quasi-one-dimensional pseudo-spin-1 systems are derived and discussed. Further discussions and future perspectives for future applications of the present results are detailed in Sec. VI.

II. GENERALIZED STUB LATTICE

Let us consider the tight-binding model of the generalized stub lattice, where the hopping amplitudes are considered real, but general otherwise. The model here is such that it converges to the SSH lattice or stub lattice for specific choices of the

hopping parameters. The tight-binding Hamiltonian H_{gs} of a generalized stub lattice [see Fig. 1(a)] is

$$H_{gs} = \sum_{n=-\infty}^{\infty} (t_1 A_n^\dagger B_n + t_2 A_n^\dagger B_{n-1} + t_3 A_n^\dagger C_n + \mu_A A_n^\dagger A_n$$
$$+ \mu_B B_n^\dagger B_n + \mu_C C_n^\dagger C_n) + \text{H.c.}, \qquad (1)$$

where $A_n^\dagger$, $B_n^\dagger$, and $C_n^\dagger$ are fermionic creation operators for electrons on site A_n, B_n, or C_n. The lattice is supposed to be infinite, i.e., n acquires all integer values. The quantities t_1, t_2, and t_3 are the real hopping amplitudes, and $\mu_{A,B,C}$ correspond to real on-site energies. The index n runs over all elementary cells through an infinite periodic lattice. The primitive translation vector is $(a, 0)$ so that the first Brillouin zone becomes $k \in [0, \frac{2\pi}{a}]$. The Fourier transform of H[1] provides us with the following operator:

$$H_{gs}(k) = \begin{pmatrix} \mu_A & t_1 + t_2 e^{-ika} & t_3 \\ t_1 + t_2 e^{ika} & \mu_B & 0 \\ t_3 & 0 & \mu_C \end{pmatrix}, \qquad (2)$$

together with the secular equation $\det[H_{gs}(k) - \lambda] = 0$, which reads as

$$(\lambda - \mu_B) t_3^2 + (\lambda - \mu_C)\big[t_1^2 + t_2^2 - (\lambda - \mu_A)(\lambda - \mu_B)$$
$$+ 2 t_1 t_2 \cos ak\big] = 0. \qquad (3)$$

Although the latter can be solved for any λ (for more details, see [55]), we are interested in the configuration where the flat

---

[1]This is equivalent to writing the operator in the basis of the states with fixed quasimomentum $|X\rangle = \sum_m e^{ikam}|X, m\rangle$, $X = A, B, C$, where $|X, m\rangle$ represents the occupation of position X in the mth elementary cell, and m counts the elementary cells.

band is present. Indeed, this occurs for

$$\mu_B = \mu_C, \tag{4}$$

which, henceforth, is the case under consideration. This leads to the dispersion relations of the form

$$E_{fb} = \mu_C,$$
$$E_\pm = \frac{\mu_A + \mu_C}{2}$$
$$\pm \sqrt{t_1^2 + t_2^2 + t_3^2 + \frac{(\mu_A - \mu_C)^2}{4} + 2t_1 t_2 \cos ka}. \tag{5}$$

From the latter, it is worth remarking that dispersion bands never touch, i.e., the band structure is always gapped. This is a stark difference with respect to other flat-band systems such as

the two-dimensional Lieb lattice [55], where vanishing next-nearest neighbors close the band gap. Furthermore, the trimer SSH model [16] does not hold a flat band in its spectrum.

Our model can be reduced to a couple of special cases when the parameters are fixed correspondingly. That is, for $t_3 = 0$, the C atoms are effectively isolated from the linear chain formed by A and B atoms. The C atoms host the flat-band states with energy μ_C. These states are strongly localized at the C atoms as there is no interaction with other atoms. In turn, for $t_1 \neq t_2$, the linear chain of $A - B$ atoms coincides with an infinite SSH model. The case $t_1 = t_2 = t_3$ reproduces the stub lattice. The band structure of the system is illustrated in Fig. 1(b).

The energy band E_+ (E_-) has its minimum (maximum) at $K = \frac{\pi}{a}$. Expanding E_+ around this point, $k = K + \delta k$, we get

$$E_\pm = \frac{\mu_A + \mu_C}{2} \pm \sqrt{\sum_{j=1}^{3} t_j^2 + \frac{(\mu_A - \mu_C)^2}{4} - 2t_1 t_2 (1 - a^2 \delta k^2 + a^4 \delta k^4 + \cdots)}.$$

When the momentum k is considered in the range where the quartic and higher terms in the expansion are negligible,

$$a^{2n} \delta k^{2n} \sim 0, \quad n \geqslant 2,$$

the dispersion relation turns into the expression known for massive one-dimensional Dirac fermions. By expanding the Hamiltonian (2) at K up to the first order in δk, we get the Dirac-type operator for

$$H_{gs}(K + \delta k) \sim \begin{pmatrix} \mu_A & t_1 - t_2 + iat_2\delta k & t_3 \\ t_1 - t_2 - iat_2\delta k & \mu_C & 0 \\ t_3 & 0 & \mu_C \end{pmatrix}, \tag{6}$$

which acts, in general, on three-component wave functions $\Psi \in \mathbb{C}^3$. For the sake of simplicity, it is more convenient to make the additional transformation $(\psi_1, \psi_2, \psi_3) \rightarrow (\psi_1, i\psi_2, i\psi_3)$. The resulting operator in coordinate representation reads as

$$h_{gs} = \begin{pmatrix} \mu_A & -i(t_1 - t_2) - iat_2\partial_x & -it_3 \\ i(t_1 - t_2) - iat_2\partial_x & \mu_C & 0 \\ it_3 & 0 & \mu_C \end{pmatrix}. \tag{7}$$

There are situations where the Dirac equation does not provide a reasonable approximation of low-energy dynamics. It can happen when the energy gap is so large that the admissible energies are already out of the range where a linear approximation of dispersion would be faithful. In our models, we assume that a reasonable control over the parameters can be reached, e.g., by performing the experiments on the optical lattices, which makes it possible to stay within the range of energies where the Dirac approximation works well.

In the next section, we will present the method that allows one to construct (7) with possibly inhomogeneous hopping t_1 and t_3 and facilitate the calculation of the associated eigenstates.

III. COUPLING VIA DARBOUX TRANSFORMATION

Let us start the section with a brief review of the Darboux transformation for Dirac-type operators of the form $H = -i\gamma \partial_x + V$, where γ and V can be generic $N \times N$ matrices. The Darboux transformation for $N = 2$ was discussed in [32], while the general case was considered in [33]. In general, the Darboux transformation relates the initially known stationary equation $(H - \epsilon)\Psi = 0$ with the new unknown equation $(\widetilde{H} - \epsilon)\widetilde{\Psi} = 0$, where $\widetilde{H} = -i\gamma \partial_x + \widetilde{V}$ is also a Dirac-type operator with an altered potential term. Furthermore, the transformation maps the solutions of the first equation into the solutions of the second equation. The latter is not necessarily a one-to-one mapping and is achieved through a first-order and nonunitary differential operator L, the exact form of which is shown below.

The transformation is based on N eigenstates Ψ_a, $a = 1, 2, \ldots, N$, of H, $(H - \lambda_a)\Psi_a = 0$. The eigenstates are used to compose an $N \times N$ matrix, $U = (\Psi_1 \ \Psi_2 \ \cdots \ \Psi_N)$. There holds

$$HU = U\Lambda, \quad \Lambda = \text{diag}\{\lambda_1, \lambda_2, \ldots, \lambda_N\}, \tag{8}$$

so that we can define the new Dirac-type operator,

$$\widetilde{H} = -i\gamma \partial_x + \widetilde{V} = -i\gamma \partial_x + V - \delta V, \quad \delta V = i[\gamma, U_x U^{-1}], \tag{9}$$

with $U_x \equiv \partial_x U$. The latter is related with H through the intertwining relation $LH = \widetilde{H}L$, where L is the first-order differential operator,

$$L = iUP_x U^{-1} \equiv \partial_x - U_x U^{-1}, \tag{10}$$

with $P_x \equiv -i\partial_x$ the momentum operator. Here, the operator L effectively maps the eigenstates of H into the eigenstates of $\widetilde{H}$, with the exception of the states Ψ_a, $a = 1, \ldots, N$, that belong to the kernel of L. Indeed, there holds

$$(H - \epsilon)\Psi = 0 \implies (\widetilde{H} - \epsilon)\widetilde{\Psi} = 0, \quad \widetilde{\Psi} = L\Psi. \tag{11}$$

The Hamiltonian $\widetilde{H}$ can have the new bound states of energies λ_1, λ_2. $\widetilde{H}(U^\dagger)^{-1} = (U^\dagger)^{-1}\Lambda$. The columns of $(U^\dagger)^{-1}$ correspond to formal eigenstates of $\widetilde{H}$. When the jth column of the latter matrix is square integrable, it forms the bound state of $\widetilde{H}$ with energy λ_j; see [32].

Let us consider a generic, one-dimensional pseudo-spin-1/2 Dirac system described by the following stationary equation:

$$H_{1/2}\Psi = \begin{pmatrix} m+v & -i\partial_x - iA \\ -i\partial_x + iA & -m+v \end{pmatrix}\begin{pmatrix} i\psi \\ \phi \end{pmatrix} = \epsilon\begin{pmatrix} i\psi \\ \phi \end{pmatrix}, \quad (12)$$

where $m = m(x)$, $v = v(x)$, and $A = A(x)$ are real functions so that $H_{1/2}$ is Hermitian. We assume that it is possible to find formal solutions of the equation for any real ϵ.

We trivially extend $H_{1/2}$ by an additional degree of freedom so that the new operator has the form

$$H_1 = \begin{pmatrix} m+v & -i\partial_x - iA & 0 \\ -i\partial_x + iA & -m+v & 0 \\ 0 & 0 & \lambda \end{pmatrix}. \quad (13)$$

This represents a system where two subsystems coexist without any mutual interaction. In one of them, the dynamics is driven by $H_{1/2}$, while in the second one, the dynamics is frozen as the energy operator is constant.

It is straightforward to find the eigenvectors of the extended operator H_1 from the eigenvectors of $H_{1/2}$. We shall use them to perform the supersymmetric (susy) transformation of H_1. In order to do so, we fix the matrix U [see (8)] in the following manner:

$$U = \begin{pmatrix} i\psi_0 & i\psi_1 & i\psi_2 \\ \phi_0 & \phi_1 & \phi_2 \\ 0 & \xi_1 & \xi_2 \end{pmatrix}, \quad H_1 U = U\begin{pmatrix} \epsilon & 0 & 0 \\ 0 & \lambda & 0 \\ 0 & 0 & \lambda \end{pmatrix},$$

$$\epsilon, \lambda \in \mathbb{R}. \quad (14)$$

The columns of U are formed by the eigenvectors corresponding to the eigenvalues ϵ or λ, respectively. The components $\psi_a, \phi_a, a = 1, 2, 3$, and ξ_1 and ξ_2 can be fixed as real-valued functions. The functions ξ_1 and ξ_2 can be arbitrary, but they should not be zero identically as the transformed Hamiltonian with coupled subsystems could not be Hermitian in that case; see the Appendix.

With the matrix U fixed, we can construct L and $\widetilde{H}_1$ through (10) and (13), such that the intertwining relation is satisfied. The new potential $\widetilde{V}_1$ is not Hermitian in general. Nevertheless, we can exploit the freedom in the choice of the functions ξ_1 and ξ_2 in order to recover the Hermiticity of $\widetilde{V}_1$ in (13). To this end, it is sufficient to fix ξ_1 in the following manner:

$$\xi_1 = \xi_2\left(c_1 - \int \frac{(\epsilon - \lambda)(\phi_2\psi_1 - \phi_1\psi_2)}{\xi_2^2}dx\right)$$

$$= \xi_2\left(c_1 - \int \frac{(\epsilon - \lambda)W_0}{\xi_2^2}dx\right), \quad (15)$$

with c_1 a real integration constant. It is worth noticing that $W_0 \equiv \phi_2\psi_1 - \phi_1\psi_2$ is a real constant as well. Indeed, the relation $\partial_x W_0 = 0$ can be derived when taking into account that $(\psi_1, \phi_1)^t$ and $(\psi_2, \phi_2)^t$ are eigenvectors of $H_{1/2}$ corresponding to the same eigenvalue.

The new Hamiltonian $\widetilde{H}_1$ defined in (13) has the following form:

$$\widetilde{H}_1 = \begin{pmatrix} 0 & -i\partial_x & 0 \\ -i\partial_x & 0 & 0 \\ 0 & 0 & 0 \end{pmatrix} + \widetilde{V},$$

$$\widetilde{V} = \begin{pmatrix} \widetilde{V}_{11} + v & -i\widetilde{V}_{12} & -i\widetilde{V}_{13} \\ i\widetilde{V}_{12} & -\widetilde{V}_{11} + v & \widetilde{V}_{23} \\ i\widetilde{V}_{13} & \widetilde{V}_{23} & \lambda \end{pmatrix}, \quad (16)$$

where

$$\widetilde{V}_{12} = -A + (\epsilon - \lambda)\frac{\psi_0(\xi_2\psi_1 - \xi_1\psi_2) - \phi_0(\xi_2\phi_1 - \xi_1\phi_2)}{\psi_0(\xi_2\phi_1 - \xi_1\phi_2) - \phi_0(\xi_2\psi_1 - \xi_1\psi_2)},$$

$$\widetilde{V}_{13} = \frac{(\epsilon - \lambda)\psi_0(\phi_1\psi_2 - \phi_2\psi_1)}{\psi_0(\xi_2\phi_1 - \xi_1\phi_2) - \phi_0(\xi_2\psi_1 - \xi_1\psi_2)}$$

$$= -\frac{(\epsilon - \lambda)\psi_0 W_0}{\psi_0(\xi_2\phi_1 - \xi_1\phi_2) - \phi_0(\xi_2\psi_1 - \xi_1\psi_2)},$$

$$\widetilde{V}_{23} = -\frac{(\epsilon - \lambda)\phi_0(\phi_1\psi_2 - \phi_2\psi_1)}{\psi_0(\xi_2\phi_1 - \xi_1\phi_2) - \phi_0(\xi_2\psi_1 - \xi_1\psi_2)},$$

$$\widetilde{V}_{11} = -m + (\epsilon - \lambda)\frac{\psi_0(\xi_2\phi_1 - \xi_1\phi_2) + \phi_0(\xi_2\psi_1 - \xi_1\psi_2)}{\psi_0(\xi_2\phi_1 - \xi_1\phi_2) - \phi_0(\xi_2\psi_1 - \xi_1\psi_2)}. \quad (17)$$

All the nonvanishing components (17) of the potential $\widetilde{V}_1$ share the same denominator, $d(x) := \psi_0(\xi_2\phi_1 - \xi_1\phi_2) - \phi_0(\xi_2\psi_1 - \xi_1\psi_2)$, proportional to $\det U$. The zeros of d introduce additional singularities into $\widetilde{V}_1$. Such a situation would be undesirable as it would be necessary to introduce additional boundary conditions at the singularities. The additional boundary conditions could compromise the calculation of physically relevant eigenstates of $\widetilde{H}_1$. Indeed, physical eigenstates of H_1 could be mapped into the formal eigenstates of $\widetilde{H}_1$ that would not belong to its domain. Therefore, the elements of the matrix U should be set such that d is a nodeless function.

The components U are not independent. Indeed, ξ_1 is given in terms of ξ_2; see (15). The functions ψ_a can be expressed in terms of $\phi_a, a = 0, 1, 2$, respectively,

$$\psi_a = \frac{\phi_a' + A\phi_a}{m + v - \lambda}, \quad \phi_a' \equiv \partial_x\phi_a. \quad (18)$$

Additionally, ϕ_1 can be expressed via ϕ_2 as they are two linearly independent solutions of

$$-\left[(-\partial_x + A)\frac{1}{m + v - \lambda}(\partial_x + A)\right]\phi_{1,2} + (v - m - \lambda)\phi_{1,2}$$

$$= 0. \quad (19)$$

Therefore, $d \equiv d(x)$ is determined by three functions only, $d = d(\phi_0, \phi_2, \xi_2)$, where ξ_2 is arbitrary in principle. The freedom in its choice can be exploited to keep $\widetilde{V}_1$ free of any additional singularities. We discuss the explicit choice of ξ_2 in the models presented in the next section.

The formulas (17) suggest that a major simplification of the potential $\widetilde{V}_1$ occurs when either $\psi_0 = 0$ or $\phi_0 = 0$. Then, there holds $\widetilde{V}_{13} = 0$ or $\widetilde{V}_{23} = 0$, respectively. We are interested in the latter as $\widetilde{V}_1$ acquires the form of the Dirac operator (7) in this case. Although it is not possible to set $\phi_0 = 0$ for a generic

Hamiltonian H_1, it is possible for cases where H_1 acquires the specific form

$$H_1 = \begin{pmatrix} m & -i\partial_x - iA(x) & 0 \\ -i\partial_x + iA(x) & -m & 0 \\ 0 & 0 & \lambda \end{pmatrix}, \quad (20)$$

where m is a real constant. When we fix $\epsilon = m$, we can find the corresponding eigenstate $(\psi_0, \phi_0, 0)$, where $\phi_0 = 0$ and $\psi_0 = \exp[\int A(x)dx]$. The matrix U then reads as

$$U = \begin{pmatrix} i \exp\left[\int A(x)dx\right] & i\psi_1 & i\psi_2 \\ 0 & \phi_1 & \phi_2 \\ 0 & \xi_1 & \xi_2 \end{pmatrix},$$

$$H_1 U = U \begin{pmatrix} m & 0 & 0 \\ 0 & \lambda & 0 \\ 0 & 0 & \lambda \end{pmatrix}, \quad \lambda \in \mathbb{R}. \quad (21)$$

The components of the simplified potential term $\widetilde{V}_1$

$$\widetilde{V}_1 = \begin{pmatrix} -\lambda & -i\widetilde{V}_{12} & -i\widetilde{V}_{13} \\ i\widetilde{V}_{12} & \lambda & 0 \\ i\widetilde{V}_{13} & 0 & \lambda \end{pmatrix} \quad (22)$$

are as follows:

$$\widetilde{V}_{12}(x) = -A(x) + (m - \lambda)\frac{\xi_2\psi_1 - \xi_1\psi_2}{\xi_2\phi_1 - \xi_1\phi_2},$$

$$\widetilde{V}_{13}(x) = -\frac{(m - \lambda)W_0}{\xi_2\phi_1 - \xi_1\phi_2}. \quad (23)$$

Equation (19) reduces to a Schrödinger-type equation. Assuming that ϕ_2 is fixed, we get ϕ_1 as follows:

$$\phi_1 = \phi_2\left(c_0 - \int \frac{(m - \lambda)W_0}{\phi_2^2}dx\right). \quad (24)$$

After substituting (15) and (24) into (23), we obtain the potential components,

$$\widetilde{V}_{12}(x) = -A(x) + (m - \lambda)\frac{\psi_2}{\phi_2} + \widetilde{V}_{13}\frac{\xi_2}{\phi_2}, \quad (25)$$

$$\widetilde{V}_{13}(x) = -\frac{(m - \lambda)W_0}{\xi_2\phi_2\left[\delta c + W_0(m - \lambda)\left(\int \frac{1}{\xi_2^2}dx + \int \frac{1}{\phi_2^2}dx\right)\right]},$$

$$\delta c = c_0 - c_1. \quad (26)$$

Comparing the potential terms in $\widetilde{H}_1$ with h_{gs} in (7),

$$\begin{pmatrix} -\lambda & -i\widetilde{V}_{12} - i\partial_x & -i\widetilde{V}_{13} \\ i\widetilde{V}_{12} - i\partial_x & \lambda & 0 \\ i\widetilde{V}_{13} & 0 & \lambda \end{pmatrix}$$

$$= \begin{pmatrix} \mu_A & -i(t_1 - t_2) - iat_2\partial_x & -it_3 \\ i(t_1 - t_2) - iat_2\partial_x & \mu_C & 0 \\ it_3 & 0 & \mu_C \end{pmatrix}, \quad (27)$$

we find that the two operators coincide, provided that

$$t_2 = 1/a, \quad \mu_C \equiv \lambda, \quad \mu_A = -\lambda,$$

$$t_1 \equiv 1/a + \widetilde{V}_{12}, \quad t_3 \equiv \widetilde{V}_{13}. \quad (28)$$

The hopping amplitudes t_1 and t_3 in the effective Hamiltonian $\widetilde{H}_1$ of the quasi-one-dimensional chain would be inhomogeneous. In this context, the operator H_1 described two systems without any mutual interaction. In contrast, the operator $\widetilde{H}_1$ corresponds to a qualitatively different physical reality; the two subsystems are coupled by $\widetilde{V}_{13}$. In the next section, we will apply the presented framework for the construction of two explicit models that can be matched with a decorated SSH model. We will discuss three explicit models where the inhomogeneity makes it possible to convert the SSH chain to a stub lattice locally.

IV. TUNABLE FLAT BAND IN THE GAP

Let us fix the Hamiltonian $H_{1/2}$ in (12) as the energy operator of a massive particle with pseudo-spin-1/2 under the influence of a null external magnetic field with the gauge rule $A(x) = A_0 \in \mathbb{R}$. The trivially extended operator H_1 then reads as

$$H_1 = \begin{pmatrix} m & -i\partial_x - iA_0 & 0 \\ -i\partial_x + iA_0 & -m & 0 \\ 0 & 0 & \lambda \end{pmatrix}, \quad (29)$$

where m and λ are real constants, and the corresponding eigenvectors can be found for any ϵ. In accordance with the results of the previous section, we fix $\epsilon = m$ and

$$\psi_0 = e^{A_0 x}, \quad \phi_0 = 0, \quad (H_1 - m)(i\psi_0, \phi_0, 0) = 0. \quad (30)$$

As mentioned in (18) and (19), the components $\psi_{1,2}$ and ϕ_1 can be obtained in terms of ϕ_2. We will assume that $|\lambda| \neq |m|$. Then we can write

$$\psi_{1,2} = \frac{\phi'_{1,2} + A_0\phi_1}{m - \lambda}, \quad \phi_1 = \phi_2\left(\int \frac{W_0(m - \lambda)}{\phi_2^2} + c_0\right), \quad (31)$$

where c_0 is a real constant. We used the fact that ϕ_1 and ϕ_2 have to solve the same differential equation (19) of the second order. We assume that they are linearly independent, i.e., the Wronskian W_0 of the two solutions is nonvanishing, $W_0 \neq 0$. The component ξ_1 is fixed as in (15).

The functions ϕ_2 and ξ_2 are to be selected such that the components (17) of $\widetilde{V}_1$ are free of singularities. We make the following choice:

$$\phi_2 = \cosh\kappa x, \quad \xi_2 = -\rho\cosh\kappa x,$$

$$\kappa = \sqrt{m^2 + A_0^2 - \lambda^2}, \quad \rho \in \mathbb{R}. \quad (32)$$

Here we assume that A, m, and λ are fixed such that κ is real. The matrix U than satisfies (21). The Hamiltonian $\widetilde{H}_1$ and the intertwining operator L have the following explicit forms:

$$\widetilde{H}_1 = \begin{pmatrix} 0 & -i\partial_x & 0 \\ -i\partial_x & 0 & 0 \\ 0 & 0 & 0 \end{pmatrix} + \begin{pmatrix} -\lambda & -i\widetilde{V}_{12} & -i\widetilde{V}_{13} \\ i\widetilde{V}_{12} & \lambda & 0 \\ i\widetilde{V}_{13} & 0 & \lambda \end{pmatrix}, \quad (33)$$

$$L = \partial_x - \begin{pmatrix} A & i(m + \lambda) & 0 \\ 0 & \widetilde{V}_{12} & \widetilde{V}_{13} \\ 0 & \widetilde{V}_{13} & \widetilde{V}_{12} + \frac{1 - \rho^2}{\rho}\widetilde{V}_{13} \end{pmatrix}, \quad (34)$$
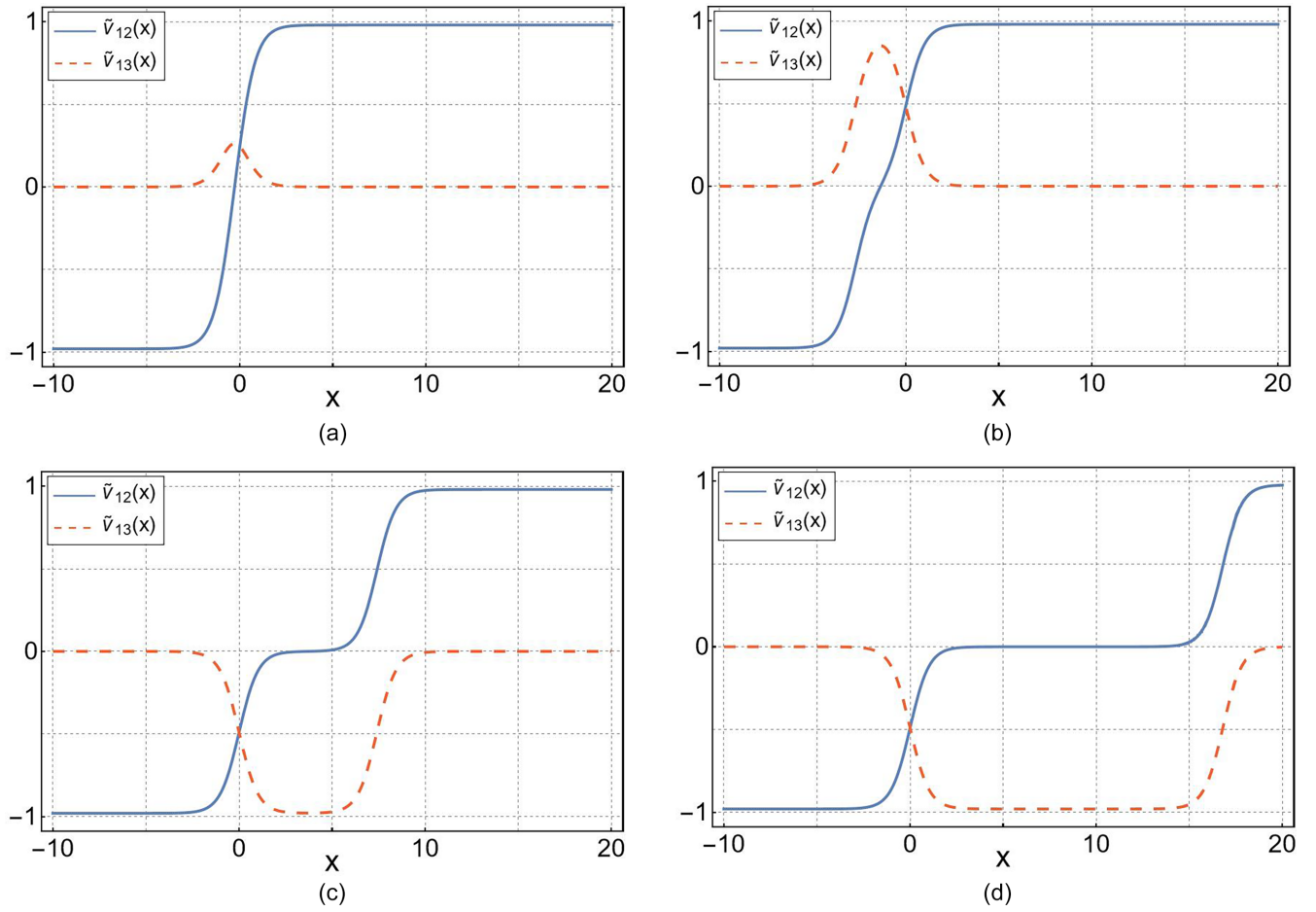
FIG. 2. Matrix potential terms $\widetilde{V}_{12}(x)$ (blue solid) and $\widetilde{V}_{13}(x)$ (red dashed) obtained from (35). Here, the parameters have been fixed to $A = m = 0.8$, $\rho = 1$, $\lambda = \frac{1}{2}\sqrt{A^2 + m^2}$, combined with (a) $\omega = 2\omega_{\text{crit}}$, (b) $\omega = (1 + 10^{-2})\omega_{\text{crit}}$, (c) $\omega = -(1 + 10^{-6})\omega_{\text{crit}}$, and (d) $\omega = -(1 + 10^{-14})\omega_{\text{crit}}$.

where

$$\widetilde{V}_{12} = \kappa \tanh \kappa x + \rho \widetilde{V}_{13}, \quad \widetilde{V}_{13} = \frac{\kappa \rho \operatorname{sech}^2 \kappa x}{\kappa \rho^2 \omega + (1 + \rho^2) \tanh \kappa x}. \tag{35}$$

Here we combined c_0, c_1, and W_0 into a single parameter ω,

$$\omega \equiv \frac{c_0 - c_1}{W_0(m - \lambda)}. \tag{36}$$

It can be concluded from (35) that both $\widetilde{V}_{12}$ and $\widetilde{V}_{13}$ are regular, provided that we fix ω such that

$$|\omega| \geqslant \omega_{\text{crit}} \equiv \frac{(1 + \rho^2)}{\rho^2 \kappa}. \tag{37}$$

For $|\omega| > \omega_{\text{crit}}$, the interaction $\widetilde{V}_{13}$ vanishes asymptotically. The potential term $\widetilde{V}_{12}$ is asymptotically constant, but it changes its sign,

$$\lim_{x \to \pm\infty} \widetilde{V}_{12} = \pm\kappa. \tag{38}$$

For most of the eligible values of either ω or λ, the term $\widetilde{V}_{13}(x)$ represents a rather narrow well or a bump, dependently on the sign of ω, whereas $\widetilde{V}_{12}(x)$ forms a smoothed potential step. When $|\omega|$ approaches ω_{crit}, the magnitude of $\widetilde{V}_{13}$ increases.

Simultaneously, it gets wider so that it resembles a smoothed rectangular well (for $\omega > 0$) or barrier (for $\omega < 0$). The potential $\widetilde{V}_{12}$ turns into a smoothed two-step barrier with an intermediate plateau. The width of the plateau is very sensitive to the proximity of $|\omega|$ to ω_{crit}; see Fig. 2 for illustration.

When $\omega = \omega_{\text{crit}}$, $\widetilde{V}_{13}$ simplifies considerably. We have

$$\widetilde{V}_{12} = \kappa \frac{\tanh \kappa x + \rho^2}{1 + \rho^2}, \quad \widetilde{V}_{13} = \frac{2\kappa \rho}{(1 + \rho^2)(1 + e^{2\kappa x})}. \tag{39}$$

The asymptotic behavior of the interactions is different in this case. We have

$$\lim_{x \to +\infty} \widetilde{V}_{12} = \kappa, \quad \lim_{x \to -\infty} \widetilde{V}_{12} = \kappa \frac{\rho^2 - 1}{1 + \rho^2}, \tag{40}$$

$$\lim_{x \to +\infty} \widetilde{V}_{13} = 0, \quad \lim_{x \to -\infty} \widetilde{V}_{13} = \frac{\kappa \rho}{1 + \rho^2}. \tag{41}$$

We can see that $\widetilde{V}_{12}$ is changing its sign asymptotically again. The interaction $\widetilde{V}_{13}$ acquires a nonzero constant value for large negative x.

The potential $\widetilde{V}_1$ can be matched with the interaction term of the quasi-one-dimensional chain (27) where the generalized stub lattice gets converted into a SSH chain with a parallel chain of noninteracting atoms. The interaction between the
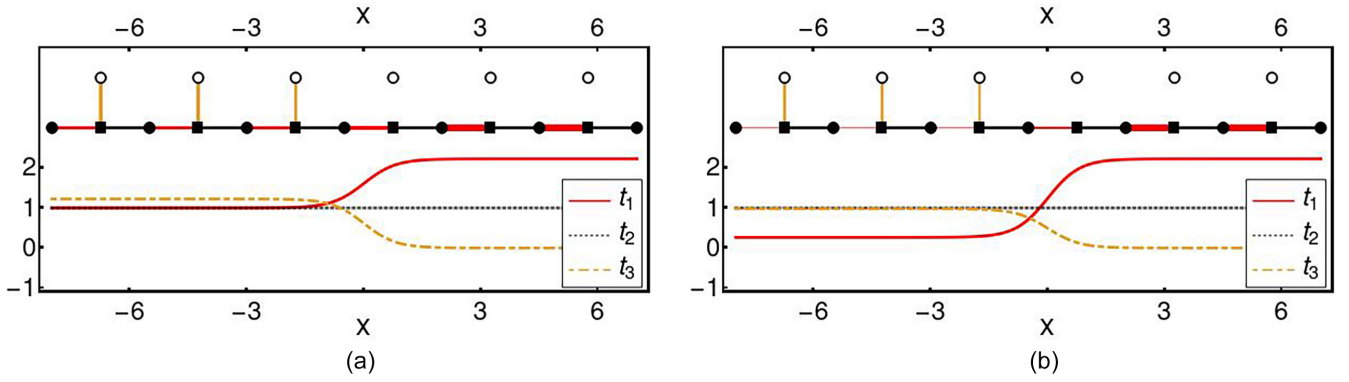
FIG. 3. Inhomogeneous hopping parameters $t_1 = t_2 + \widetilde{V}_{12}$ (red), $t_3 = \widetilde{V}_{13}$ (orange), and t_3 (gray dotted) for $\omega = \omega_c$ computed from (37), (39), and (28). We fixed $t_2 = 1$, $m = 1$, $A = 1$, $\lambda = \frac{1}{2}\sqrt{A^2 + m^2}$, and $\rho = 1$ (left) and $\rho = 0.5$ (right). Insets: The quasi-one-dimensional chain with the corresponding interactions (the thicker the line, the stronger the coupling), with t_1 red, t_2 black, and t_3 the vertical line.

two chains is localized in the case of (35), while in the case of (39), it gets extended over the half axis. The dimerization pattern on the SSH chain changes as the ratio of t_1/t_2 (where $t_1 = \widetilde{V}_{12} + t_2$) is inverted along the x axis. In this way, it resembles the SSH chains with a domain wall. Figure 3 illustrates the case $\omega = \omega_{\text{crit}}$, where a semi-infinite generalized stub lattice decomposes at the origin into an SSH chain with parallel noninteracting atoms.

As noted below (11), supersymmetric transformation can generate bound states with discrete energies in the new system. The candidates for the new bound states are formed by the columns of the matrix $(U^\dagger)^{-1}$ that satisfy

$$\widetilde{H}_1 (U^\dagger)^{-1} = (U^\dagger)^{-1} \text{diag}\{m, \lambda, \lambda\}. \tag{42}$$

The eigenstate corresponding to the eigenvalue m is not normalizable, while the other two columns are eigenvectors with the eigenvalue λ. Their explicit form and square integrability is not of our interest. The reason is that λ corresponds to the flat-band energy and, therefore, is infinitely degenerated anyway. Indeed, we can find an infinite number of independent normalizable eigenvectors of the form $L[0, 0, \xi(x)]^T$ where $||\xi|| < \infty$, with T the transposition operation.

By construction, the spectrum of $\widetilde{H}_1$ is composed of two energy bands of negative and positive energies. The energy λ of the flat band can take any value within the energy gap,

$$\sigma(\widetilde{H}_1) = \left(-\infty, -\sqrt{m^2 + A_0^2}\, \right] \cup \left[\sqrt{m^2 + A_0^2}, \infty \right) \cup \{\lambda\},$$
$$\lambda^2 < m^2 + A_0^2. \tag{43}$$

The barrier represented by $\widetilde{V}_1$ in (35) is perfectly transparent. The quasiparticles tunnel through it without being backscattered. It it reminiscent to the Klein tunneling of quasiparticles in graphene through electrostatic barriers. Here, the particles can pass through the barrier without reflection independently of their energy. It can be understood with the use of the intertwining operator L that makes it possible to map the eigenstates of H_1 into those of $\widetilde{H}_1$. The Hamiltonian H_1 corresponds to the free-particle energy operator with a constant potential. Let us suppose that its physical eigenstate $\psi_k(x) = e^{ikx}(a, b, c)^t$ corresponds to the plane waves with a fixed momentum $k \in \mathbb{R}$. The intertwining operator L converts

these states into the scattering states of $\widetilde{H}_1$. We can write

$$L\psi_k(x) = (\partial_x - U_x U^{-1}) e^{ikx}(a, b, c)^t$$
$$= e^{ikx}(ik - U_x U^{-1})(a, b, c)^t, \tag{44}$$

where a, b, c are complex-valued constant components of the three-component wave function. The matrix $U_x U^{-1}$ converges to a constant matrix for large $|x|$. Therefore, $L\psi_k(x)$, $|x| \to \infty$, acquires the form of the plane wave whose momentum is not altered by the potential barrier,

$$\lim_{x \to \pm\infty} L\psi_k(x) = e^{ikx}(\tilde{a}_\pm, \tilde{b}_\pm, \tilde{c}_\pm)^t, \quad \tilde{a}_\pm, \tilde{b}_\pm, \tilde{c}_\pm \in \mathbb{C}, \tag{45}$$

i.e., there is no backscattering.

V. COEXISTENCE OF DISCRETE AND FLAT-BAND ENERGY LEVELS

The Hamiltonian $\widetilde{H}_1$ can inherit spectral properties of the initial, uncoupled operator H_1. The latter one, by construction, shares the spectrum of $H_{1/2}$ except the flat-band energy. Therefore, the spectral design of $\widetilde{H}_1$ starts with the proper choice of $H_{1/2}$. In this section, we present the models where the flat band coexists with discrete energies. The models with one and two discrete energies are introduced. We illustrate how Darboux transformation can be used in two steps. In the first one, 2×2 Darboux transformation can generate $H_{1/2}$ with the requested structure of discrete energies. In the second step, Darboux transformation applied on 3×3 operator H_1 produces the Hamiltonian $\widetilde{H}_1$.

A. Two bound states and a flat band

In this section, we design a solvable model of a pseudo-spin-1 system with two discrete energies and a flat band in the energy spectrum. We will discuss in detail the role of the Darboux transformation at different stages of the construction.

First, we shall construct a solvable model described by a pseudo-spin-1/2 Hamiltonian that has two discrete energies in its spectrum. Let us set the initial Hamiltonian as the energy operator of a free-particle system as

$$H_{1/2} = -i\sigma_1 \partial_x + m_0\sigma_2, \quad m_0 > 0. \tag{46}$$

The spectrum of $H_{1/2}$ consists of two bands divided by the energy gap that stretches between $\pm m_0$. Darboux transformation can be used to convert $H_{1/2}$ into the new pseudo-spin-1/2 Hamiltonian that would possess two discrete energies. We can rely here on the existing results. Solvable systems constructed from the free-particle model via Darboux transformation were discussed in [41,43], where models with diverse configurations of discrete energies within the energy gap were presented.

We demand that there are two discrete real energies λ_0 and $-\lambda_0$ in the new system. In order to construct such a Hamiltonian, we fix the matrix $U_{1/2}$ in the following manner (see [41] for more details):

$$H_{1/2}U_{1/2} = U_{1/2}\begin{pmatrix} \lambda_0 & 0 \\ 0 & -\lambda_0 \end{pmatrix}, \quad U_{1/2} = \begin{pmatrix} u_{11} & -iu_{11} \\ iu_{21} & -u_{21} \end{pmatrix},$$

where $u_{11} = \cosh k_0 x$, $u_{21} = \cosh(k_0 x + a_0)$, and

$$k_0 = \sqrt{m_0^2 - \lambda_0^2}, \quad a_0 = \frac{1}{2}\ln\frac{m_0 - k_0}{m_0 + k_0},$$

$$|\lambda_0| < |m_0|, \quad \lambda_0, m_0 \in \mathbb{R}. \tag{48}$$

The intertwining operator $L_{1/2}$ and the new Hamiltonian $\widetilde{H}_{1/2}$ can be written as

$$\widetilde{H}_{1/2} = -i\sigma_1\partial_x + A(x)\sigma_2,$$

$$L_{1/2} = \partial_x - k_0\begin{pmatrix} \tanh k_0 x & 0 \\ 0 & \tanh(k_0 x + a_0) \end{pmatrix},$$

$$A(x) = [m_0 - k_0\tanh k_0 x + k_0\tanh(k_0 x + a_0)]. \tag{49}$$

They satisfy

$$L_{1/2}H_{1/2} = \widetilde{H}_{1/2}L_{1/2}. \tag{50}$$

The two linearly independent eigenstates of $H_{1/2}$ corresponding to the eigenvalue λ are

$$F(\lambda) = (f_1, f_2)^t = (-i(m_0\cosh xk + k\sinh kx), \lambda\cosh kx)^t, \tag{51}$$

$$G(\lambda) = (g_1, g_2)^t = (-i(m_0\sinh xk + k\cosh kx), \lambda\sinh kx)^t,$$

$$k = \sqrt{m_0^2 - \lambda^2}. \tag{52}$$

They satisfy

$$(H_{1/2} - \lambda)F(\lambda) = 0, \quad (H_{1/2} - \lambda)G(\lambda) = 0, \quad \lambda \in \mathbb{C}. \tag{53}$$

The eigenstates $\widetilde{F}(\lambda)$ and $\widetilde{G}(\lambda)$ of $\widetilde{H}_{1/2}$ for an eigenenergy $\lambda \neq \lambda_0$ can be found with help of the intertwining operator $L_{1/2}$,

$$(\widetilde{H}_{1/2} - \lambda)\widetilde{F}(\lambda) = 0, \quad \widetilde{F}(\lambda) \equiv L_{1/2}F(\lambda) = (\widetilde{f}_1, \widetilde{f}_2)^t, \tag{54}$$

$$(\widetilde{H}_{1/2} - \lambda)\widetilde{G}(\lambda) = 0, \quad \widetilde{G}(\lambda) \equiv L_{1/2}G(\lambda) = (\widetilde{g}_1, \widetilde{g}_2)^t. \tag{55}$$

The Hamiltonian $\widetilde{H}_{1/2}$ has two square integrable bound states $v^\pm$ with energy $\pm\lambda_0$ that form the columns of the matrix $(U_{1/2}^\dagger)^{-1}$ [see (42)],

$$\widetilde{H}_{1/2}v^\pm = \pm\lambda_0 v^\pm,$$

$$v^\pm = (v_1^\pm, v_2^\pm)^t = [\operatorname{sech}k_0 x, \pm i\operatorname{sech}(k_0 x + a_0)]^t. \tag{56}$$

Therefore, we constructed the operator $\widetilde{H}_{1/2}$ with the two discrete energies in the spectrum.

Now, we use the operator $\widetilde{H}_{1/2}$ to define the extended operator H_1 [see (20)],

$$H_1 = \begin{pmatrix} 0 & -i\partial_x - iA(x) & 0 \\ -i\partial_x + iA(x) & 0 & 0 \\ 0 & 0 & \lambda \end{pmatrix}, \quad |\lambda| < \lambda_0. \tag{57}$$

Darboux transformation L of the extended system is defined in terms of 3×3 matrix U; see (10) and (21). We fix the components of U in terms of solutions $\widetilde{F}(\lambda)$ and $\widetilde{G}(\lambda)$ for a given λ, $|\lambda| < \lambda_0$, in the following manner:

$$\psi_0 = i\,e^{\int A(x)dx}, \quad \psi_1 = -i\widetilde{g}_1, \quad \phi_1 = \widetilde{g}_2, \quad \psi_2 = -i\widetilde{f}_1,$$

$$\phi_2 = \widetilde{f}_2, \quad \xi_1 = \frac{\lambda^2\sqrt{m_0^2 - \lambda^2}(\lambda_0^2 - \lambda^2)}{\kappa\,\rho}\sinh\kappa x,$$

$$\xi_2 = \rho\cosh\kappa x, \quad |\lambda| < |\lambda_0|. \tag{58}$$

Then it satisfies $H_1 U = U\begin{pmatrix} 0 & 0 & 0 \\ 0 & \lambda & 0 \\ 0 & 0 & \lambda \end{pmatrix}$. The Hamiltonian $\widetilde{H}_1$ can be constructed as in (9). It inherits the discrete energies $\pm\lambda_0$ of H_1. The corresponding bound states $\widetilde{w}^\pm$ can be found with the help of the intertwining operator L,

$$\widetilde{w}^\pm = L(v_1^\pm, v_2^\pm, 0)^t, \quad \widetilde{H}_1\widetilde{w}^\pm = \pm\lambda\widetilde{w}^\pm. \tag{59}$$

The parameters ρ and κ of the flat-band solution can be arbitrary in principle. Substituting (58) into (23), the elements $\widetilde{V}_{12}$ and $\widetilde{V}_{13}$ of the potential of the new Hamiltonian $\widetilde{H}_1$ are represented by rather extensive formulas that we will not explicitly present here. The numerical tests reveal the range of ρ and κ where $\widetilde{V}_{12}$ and $\widetilde{V}_{13}$ are regular; see Fig. 4(a).

Nevertheless, the model gets remarkably simplified when ρ and κ are fixed as follows:

$$\kappa = \sqrt{m_0^2 - \lambda^2}, \quad \rho = \lambda\sqrt{\lambda_0^2 - \lambda^2}. \tag{60}$$

Then the intertwining operators $\widetilde{H}_1$ and L acquire a particularly simple form,

$$\widetilde{H}_1 = \begin{pmatrix} 0 & -i\partial_x & 0 \\ -i\partial_x & 0 & 0 \\ 0 & 0 & 0 \end{pmatrix} + \begin{pmatrix} -\lambda & -i\widetilde{V}_{12} & -i\widetilde{V}_{13} \\ i\widetilde{V}_{12} & \lambda & 0 \\ i\widetilde{V}_{13} & 0 & \lambda \end{pmatrix},$$

$$L = \partial_x - \begin{pmatrix} A(x) & i\lambda & 0 \\ 0 & \widetilde{V}_{12} & \widetilde{V}_{13} \\ 0 & \widetilde{V}_{13} & -\widetilde{V}_{12} \end{pmatrix}, \tag{61}$$

where

$$\widetilde{V}_{12} = -k_0\tanh(k_0 x + a_0), \quad \widetilde{V}_{13} = \sqrt{\lambda_0^2 - \lambda^2}, \tag{62}$$

and $A(x)$ is defined in (49). We can see that the dimerization pattern of the SSH chain undergoes the change at $x = -a_0/k_0$. The SSH chain gets coupled with the parallel chain of atoms by $\widetilde{V}_{13}$ that acquires a constant value. The components $\widetilde{V}_{12}$ and $\widetilde{V}_{13}$ are plotted in Fig. 4(b). The atomic chain with the corresponding hopping parameters is illustrated in Fig. 5.
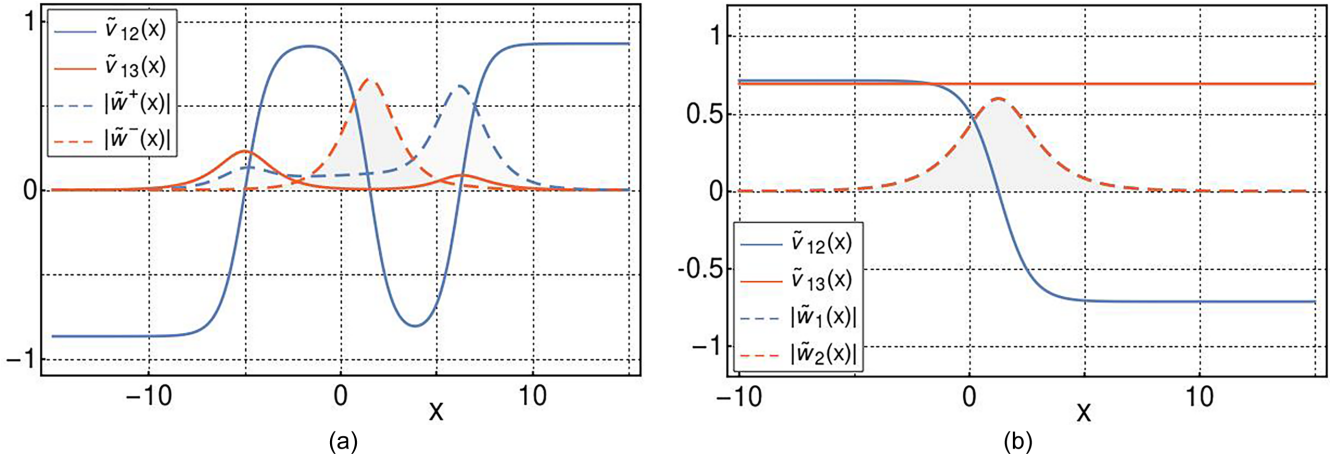
FIG. 4. Matrix potential elements $\widetilde{V}_{12}(x)$, $\widetilde{V}_{13}(x)$, and the probability densities of the (normalized) bound states $|w^{\pm}|$; see the insets for the color scheme. The parameters have been fixed as (a) $m_0 = 1$, $\lambda_0 = 0.5$, $\lambda = 0.499$, $\kappa = 0.04$, $\rho = 0.06$, and (b) κ and ρ are fixed as in (60), $m_0 = 1$, $\lambda_0 = 0.7$, $\lambda = 0.1$.

With the current choice (60) of κ and ρ, the bound states (59) are

$$\widetilde{w}^{\pm} = L(v_1^{\pm}, v_2^{\pm}, 0) = \left[\widetilde{w}_1^{\pm}, 0, \pm i \sqrt{\lambda_0^2 - \lambda} \operatorname{sech}(a_0 + k_0 x)\right], \tag{63}$$

where

$$\widetilde{w}_1^{\pm} = \frac{m_0 \lambda \mp (2k_0^2 + \lambda^2) \cosh(a_0) \mp 2k_0 m_0 \sinh(a_0)}{2\lambda \cosh k_0 x \cosh^2(k_0 x + a_0)} \tag{64}$$

$$+ \frac{\lambda(m_0 \cosh 2xk_0 - k_0 \sinh 2xk_0) - \lambda^2 \cosh(2k_0 x + a_0)}{2\lambda \cosh k_0 x \cosh^2(k_0 x + a_0)}. \tag{65}$$

The other eigenstates of $\widetilde{H}_1$ for eigenvalues λ can be found from those of $\widetilde{H}_{1/2}$ [see (55)],

$$\widetilde{\mathcal{F}} = L(\widetilde{f}_1, \widetilde{f}_2, 0)^t, \quad \widetilde{\mathcal{G}} = L(\widetilde{g}_1, \widetilde{g}_2, 0)^t. \tag{66}$$

Discussion of the scattering properties of the model with the potential (75) can be conducted in close analogy with the previous model. The matrix $U_x U^{-1}$ in the operator $L = \partial_x - U_x U^{-1}$ tends asymptotically to a constant matrix and, therefore, the operator L cannot change the momentum of the plane wave that corresponds to the scattering state of H_1.
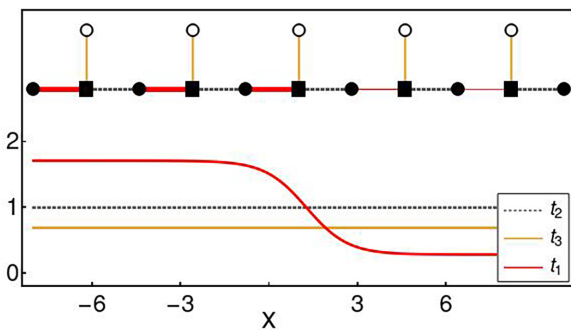

FIG. 5. Inhomogeneous hopping parameters $t_1 = t_2 + \widetilde{V}_{12}$ (red), $t_3 = \widetilde{V}_{13}$ (orange), and t_3 (gray dotted) as given by (61). The parameters are fixed as $\lambda_0 = 0.7$, $m_0 = 1$, and $\lambda = 0.1$.

Therefore, the current setting described by $\widetilde{H}_1$ is also free of backscattering.

In the construction, we used Darboux transformation at two different occasions. First, it was used to derive pseudo-spin-$1/2$ Hamiltonian $\widetilde{H}_{1/2}$ with the requested discrete energies. In that case, the intertwining operator $L_{1/2}$ was represented by the 2×2 matrix operator (49). Then we applied another Darboux transformation given in terms of the 3×3 operator L. In the specific case (60), it acquired a compact form (61). It provided us with the Hamiltonian $\widetilde{H}_1$. It is worth noticing in this context that the two intertwining relations mediated by $L_{1/2}$ and L can be brought into a compatible form by an extension of the operator $L_{1/2}$. Indeed, the intertwining relation (50) can be written as

$$\begin{pmatrix} L_{1/2} & 0 \\ 0 & 1 \end{pmatrix} \begin{pmatrix} H_{1/2} & 0 \\ 0 & \lambda \end{pmatrix} = \begin{pmatrix} \widetilde{H}_{1/2} & 0 \\ 0 & \lambda \end{pmatrix} \begin{pmatrix} L_{1/2} & 0 \\ 0 & 1 \end{pmatrix}. \tag{67}$$

Then it is possible to write a single intertwining relation that connects the trivially extended initial Hamiltonian $\begin{pmatrix} H_{1/2} & 0 \\ 0 & \lambda \end{pmatrix}$ and the target Hamiltonian $\widetilde{H}_1$,

$$\mathcal{L} \begin{pmatrix} H_{1/2} & 0 \\ 0 & \lambda \end{pmatrix} = \widetilde{H}_1 \mathcal{L}, \quad \mathcal{L} = L \begin{pmatrix} L_{1/2} & 0 \\ 0 & 1 \end{pmatrix}. \tag{68}$$

B. Flat band and a single bound state

In this case, we shall consider the model with a single discrete energy and a flat-band energy. Following the strategy explained in the previous section, we shall select the Hamiltonian $H_{1/2}$ such that it has one discrete energy in the energy gap. Here we shall use the results of [43,56], where such an operator was constructed via Darboux transformation and possessed the vector potential $A(x) = m \tanh mx$. The trivially extended operator H_1 then reads as

$$H_1 = \begin{pmatrix} M & -i\partial_x - im \tanh mx & 0 \\ -i\partial_x + im \tanh mx & -M & 0 \\ 0 & 0 & \lambda \end{pmatrix}, \tag{69}$$

where M, m, and λ are real constants. The stationary equation $H_1\Psi = \epsilon\Psi$ is exactly solvable for any ϵ. Indeed, fixing the wave function $\Psi = (\psi, \phi, 0)$ and $|\epsilon| \neq M$, the stationary equation decouples into $\phi = -i\frac{\partial_x - A}{E + M}\psi$ and $(-\partial_x^2 - \epsilon^2 + M^2 + m^2)\psi = 0$. Hence, the upper component is the eigenstate of the Schrödinger Hamiltonian of the free particle. This is due to the fact that the potential term in (69) is related to the reflectionless Pöschl-Teller model[2]; see [43,56]. The operator H_1 has a square integrable bound state Ψ_{-M} with energy $-M$,

$$H_1\Psi_{-M} = -M\Psi_{-M}, \quad \Psi_{-M} = (0, \text{sech } mx, 0)^t. \quad (70)$$

The elements of the matrix U are fixed in the following manner:

$$\psi_0 = \cosh mx, \quad \psi_1 = -\mu k\sqrt{m^2 - k^2}(\cosh kx + c_0 \sinh kx),$$

$$\psi_2 = -\mu k\sqrt{m^2 - k^2}\sinh kx, \quad (71)$$

together with

$$\xi_2 = \cosh kx. \quad (72)$$

The parameter μ controls the reality of these functions, i.e., $\mu = 1$ for $k^2 < m^2$ and $\mu = -i$ for $k^2 > m^2$. The components ϕ_1 and ϕ_2 can be calculated from $\phi_a = -i\frac{\partial_x - A}{E + M}\psi_a$, with $a = 1, 2$. Furthermore, we fix the flat-band energy as

$$\lambda = \sqrt{M^2 + m^2 - k^2}. \quad (73)$$

The matrix U satisfies the relation

$$H_1 U = U \begin{pmatrix} M & 0 & 0 \\ 0 & \lambda & 0 \\ 0 & 0 & \lambda \end{pmatrix}, \quad (74)$$

so that Eq. (17) renders the potential components

$$\widetilde{V}_{11} = -\lambda, \quad (75)$$

$$\widetilde{V}_{12} = -m\tanh mx + (k^2 - m^2)$$
$$\times \frac{1 + \tanh kx[\delta c - k^2(M - \lambda)^2\mu^2 \tanh kx]}{d(x)}, \quad (76)$$

$$\widetilde{V}_{13} = (M - \lambda)\frac{\mu\sqrt{m^2 - k^2}\,k^2\,\text{sech}^2 kx}{d(x)}, \quad \delta c = c_0 - c_1, \quad (77)$$

where

$$d(x) = \delta c(k - m\tanh kx\tanh mx) + k\tanh kx - m\tanh mx \quad (78)$$

$$-k^2\mu^2(M - \lambda)^2 \tanh kx\,(k - m\tanh kx\tanh mx). \quad (79)$$

We shall fix the parameters such that $d(x)$ is nonvanishing for $x \in \mathbb{R}$ in order to keep the potential regular. The function $d(x)$ is linear in δc. The terms that do not depend on δc are bounded. Let us fix

$$k > m > 0, \quad \mu = -i.$$

Then the coefficient of δc is strictly positive and we can always fix δc such that the first term of $d(x)$ is greater than

_____

[2]The lower component ϕ of H_1 has to satisfy the Schrödinger equation for the Pöschl-Teller model.

the sum of the remaining terms. In this way, we can keep $d(x) > 0$.

We are interested in the critical value of δc. We have

$$d(x) > 0 \Leftrightarrow \delta c > \frac{m\tanh mx - k\tanh kx}{(k - m\tanh kx\tanh mx)}$$
$$+ k^2\mu^2(M^2 - \lambda^2)\tanh kx \equiv: w(x). \quad (80)$$

We find that $w(x)$ is an odd and strictly decreasing function,

$$\partial_x w(x)$$
$$= -k^3\text{sech}^2 kx\left[\frac{k^2 - m^2}{k^2(k - m\tanh kx\tanh mx)^2} + (M - \lambda)^2\right]. \quad (81)$$

We define the critical value δc_{crit} as follows:

$$\delta c_{\text{crit}} \equiv \lim_{x\to-\infty} w(x) = 1 + k^2(M - \lambda)^2. \quad (82)$$

Then both $\widetilde{V}_{12}$ and $\widetilde{V}_{13}$ are regular for $|\delta c| \geqslant |\delta c_{\text{crit}}|$. The potential term $\widetilde{V}_{12}$ changes its sign asymptotically. In the limit of large $|x|$, it has the following behavior:

$$\lim_{x\to\pm\infty}\widetilde{V}_{12} = \pm k. \quad (83)$$

The explicit form of $\widetilde{V}_{12}$ and $\widetilde{V}_{13}$ for $|\delta c| > |\delta c_{\text{crit}}|$ is in (75).

When $\delta c = -\delta c_{\text{crit}}$, we have

$$\widetilde{V}_{12} = -m\tanh mx$$
$$+ \frac{(k^2 - m^2)\{1 + \tanh kx[1 + k^2(M - \lambda)^2(1 + \tanh kx)]\}}{d_c(x)}, \quad (84)$$

$$\widetilde{V}_{13} = \frac{\sqrt{m^2 - k^2}\,k^2\,\mu\,(M - \lambda)\,\text{sech}^2 kx}{d_c(x)}, \quad (85)$$

where

$$d_c(x) = k\tanh kx - m\tanh mx$$
$$+ [1 + k^2(M^2 - \lambda^2)(1 - \mu^2\tanh kx)]$$
$$\times (k - m\tanh kx\tanh mx). \quad (86)$$

The components $\widetilde{V}_{12}$ and $\widetilde{V}_{13}$ are explicitly depicted in Fig. 6. The behavior of both $\widetilde{V}_{12}$ and $\widetilde{V}_{13}$ is sensitive to the proximity of $|\delta c|$ to $|\delta c_{\text{crit}}|$. The width of the plateau in the two-step function and the width of the well increase as $|\delta c|$ tends to $|\delta c_{\text{crit}}|$. This time, the plateau corresponds to a nonvanishing energy. In Fig. 6, we present the plots of $\widetilde{V}_{12}$ and $\widetilde{V}_{13}$ for δc that is very close to δc_{crit}, but with varying m and M such that $M^2 + m^2$ is kept constant. For small values of m, $\widetilde{V}_{12}$ forms a two-step function that resembles the potential from the previous model; see Figs. 6(a) and 6(b). As m increases, a potential well in $\widetilde{V}_{12}$ is formed; see Figs. 6(c) and 6(d). In Fig. 7, there is a plot of the hopping amplitudes $t_1 = t_2 + \widetilde{V}_{12}$ and $t_3 = \widetilde{V}_{13}$ for $\delta c = \delta c_{\text{crit}}$ of the generalized stub lattice. In this figure, there is also the generalized stub lattice with hopping amplitudes t_1, t_2, and t_3, in correspondence with (27).

Like in the previous model, the intertwining operator $L = \partial_x - U_x U^{-1}$ acquires a rather simple form asymptotically as $\lim_{x\to\pm\infty} U_x U^{-1} = U_\pm$, where $U_\pm$ is a constant matrix. Therefore, the action of the L does not alter the asymptotic
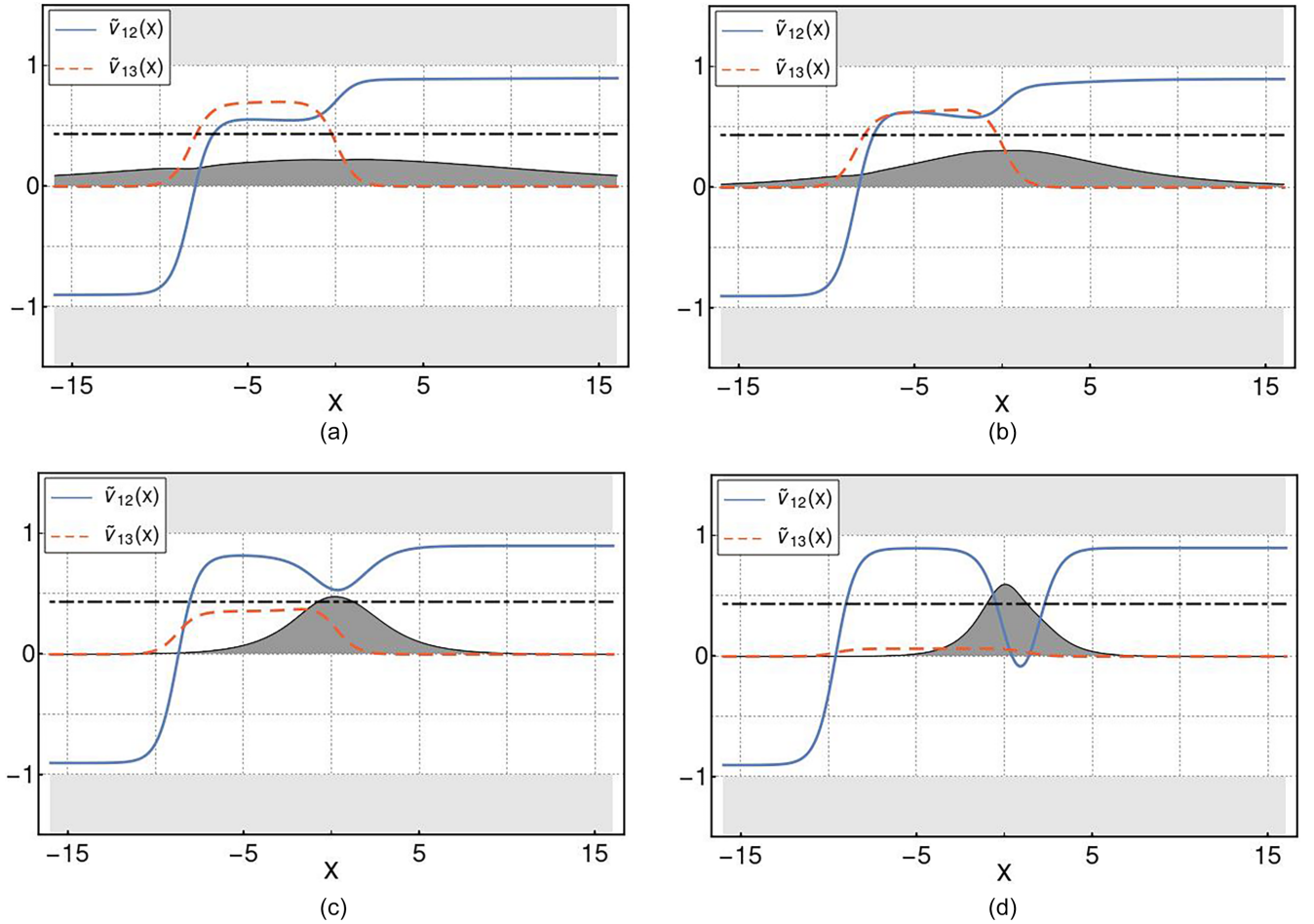
FIG. 6. Matrix potential elements $\widetilde{V}_{12}(x)$ (blue solid), $\widetilde{V}_{13}(x)$ (red dashed), and the flat-band energy level λ (dot dashed). The rest of the parameters have been fixed as $k = 0.9$, $M = \sqrt{1 - m^2}$, $\delta c = 1 + k^2(M - \lambda) + 10^{-6}$, together with (a) $m = 0.1$, (b) $m = 0.2$, (c) $m = 0.5$, and (d) $m = 0.8$. The dark-shaded curve depicts the probability density of the bound state $\tilde{\Psi}_{-M}$.

behavior of the eigenstates. It maps scattering states and bound states of H_1 into qualitatively the same states of $\widetilde{H}_1$. In particular, the Hamiltonian $\widetilde{H}_1$ inherits a bound state with energy $E = -M$. Indeed, by construction, the system has a nondegenerate energy level $E = -M$, with the corresponding bound state

$$\tilde{\Psi}_{-M} = L\,(0,\,\mathrm{sech}\,mx,\,0)^t, \quad \widetilde{H}_1 \tilde{\Psi}_{-M} = -M\tilde{\Psi}_{-M}. \quad (87)$$
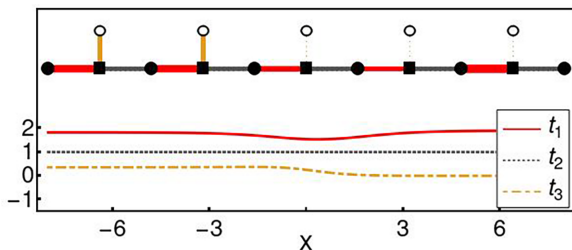

FIG. 7. $t_1 = t_2 + \widetilde{V}_{12}$ (red), $t_3 = \widetilde{V}_{13}$ (orange), and t_2 (black dotted) for $\omega = \omega_c$; see (37), (39), and (27). We fixed $t_2 = 1$, $k_0 = 0.9$, $m = 0.5$, $M = \sqrt{1 - m^2}$, $A = 1$. Inset: The quasi-one-dimensional chain with the corresponding interactions (the thicker the line, the stronger the coupling).

The density of probability of the bound state $\tilde{\Psi}_{-M}$ is plotted in Fig. 6. The spectrum of this model has the form

$$\sigma(\widetilde{H}_1) = (-\infty, -\sqrt{M^2 + m^2}\,] \cup [\sqrt{M^2 + m^2}, \infty)$$

$$\cup \{\sqrt{M^2 + m^2 - k^2}, -M\}, \quad (88)$$

where $|M| > |k| > |m|$, which is further illustrated in Fig. 8.

VI. DISCUSSION

We presented the method for the spectral design of quasi-one-dimensional crystals with a flat band that can be effectively described by the Dirac equation. Our approach is based on the susy transformation of the trivially extended pseudo-spin-one operator H_1; see (13). The latter operator is block diagonal with pseudo-spin-1/2 Hamiltonian $H_{1/2}$ and a constant on the diagonal. The operator $H_{1/2}$ governs the dynamics of a dimerized chain of atoms. The constant term represents an additional, parallel chain of atoms that are not interacting with their neighbors and host the flat-band states. The susy transformation of H_1 provides us with the operator $\widetilde{H}_1$ that already possesses nontrivial interaction between the two atomic chains; see (17) or (23). The susy transformation of H_1 is partially defined in terms of flat-band solutions. The
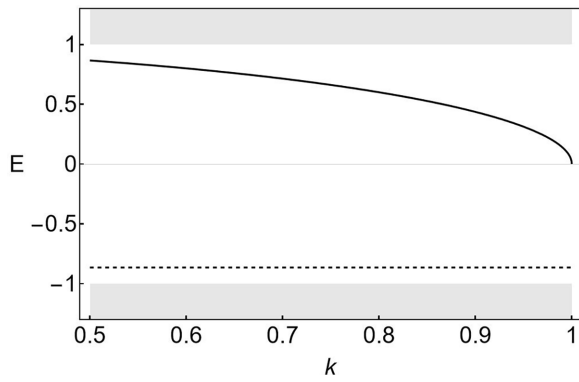
FIG. 8. Spectrum of $\widetilde{H}_1$. For each fixed value k, the two shaded bands represent the continuum. The thick black line corresponds to the flat-band energy (73) and the thin black line is the energy of the bound state $L\Psi_{-M}$. We fixed $m = 0.5$ and $M = \sqrt{1 - m^2}$.

latter functions can be selected such that $\widetilde{H}_1$ is Hermitian; see (15).

The method was explained and explicitly illustrated in three explicit models where a SSH chain interacts locally with a parallel chain of otherwise noninteracting atoms. In the models, the form of the interaction was tunable via free parameters; see Figs. 2, 4, 6. We demonstrated that in the limit where the parameters approach the critical values, the interaction approximates the piecewise constant potential; see Figs. 3, 5, 7.

The trivial extension of $H_{1/2}$ to H_1 by diagonal constant λ fixes the energy of the flat band; see (13). The remaining spectral characteristics of H_1 (and $\widetilde{H}_1$) are inherited from those of $H_{1/2}$. The spectrum of $H_{1/2}$ itself can also be adjusted by an appropriate susy transformation. The model discussed in Sec. V A exemplifies such a situation. Indeed, the block-diagonal operator in (57) can be obtained from the free-particle Hamiltonian via susy transformation that generates two discrete energies $E = \pm\lambda_0$ in the spectrum of (49). It is worth noticing that Darboux transformation applied on a pseudo-spin-1/2 system can generate up to two new bound states. When a greater number of bound states is needed, it is possible to make a sequence of Darboux transformations to get the target Hamiltonian $\widetilde{H}_{1/2}$ with the requested structure of discrete energies. Pseudo-spin-1/2 Dirac operators obtained via chains of Darboux transformations were discussed in the context of non-Hermitian optics in [42].

The models described by $\widetilde{H}_1$ also inherit scattering characteristics of H_1. In both Sec. IV and Sec. V, H_1 was fixed as the reflectionless operator. The susy partners $\widetilde{H}_1$ shared this property as they did not support any backscattering on the potential barriers. This behavior resembles Klein tunneling

that occurs in an electrostatic field; see the recent analysis in [53].

The work was inspired by [45] where a spin-one free-particle Dirac operator was transformed by supersymmetric transformation into the new ones with nontrivial potentials. In one specific case, the susy transformation resulted in decoupling of the Hamiltonian, i.e., it acquired block-diagonal form with a 2×2, spin-1/2 operator and a constant on the diagonal; see [45] for more details. The inverse approach was followed in the current article and exploited in the context of quasi-one-dimensional atomic chains. The presented construction based on susy transformation of the block-diagonal operators shares the philosophy of [57], where the interaction between uncoupled systems was induced via unitary transformations.

The presented approach to the spectral design of quasi-one-dimensional systems with flat bands is very flexible. It is straightforward to adjust it for the construction of quasi-one-dimensional systems with a higher number of flat bands and/or higher number of atoms in the elementary cell of the dimerized chain. The number of flat bands as well as their energies can be easily controlled by the addition of non-interacting parallel atomic chains to the initial Hamiltonian $H_{1/2}$, i.e., via its trivial extension by a corresponding number of diagonal constant terms. The susy transformation would generate the coupling between the original SSH-type chain(s) and the other, initially noninteracting, chains. It would also be possible to consider the effects of a magnetic field that would alter the phase of the hopping parameters. It is worth noticing in this context that the generation of the synthetic magnetic field for optical lattices was proposed in [17] and [23]. Analysis of boundary effects on a finite lattice with the use of the supersymmetric transformation represents another interesting research direction as the boundary effects can play a major role, e.g., in topological properties of the atomic chains [48]. It would also be interesting to apply this approach in the analysis of the systems with quasibound states. Nevertheless, analysis of these topics goes beyond the scope of the present work and should be reported elsewhere.

APPENDIX: ON THE STRUCTURE OF THE MATRIX U

Let us define the following set of 3×3 matrices:

$$\mathbb{M} = \left\{ M = \begin{pmatrix} \mathbb{B} & \mathbf{b} \\ \mathbf{0} & \xi \end{pmatrix}, \quad \mathbb{B} \in \mathbb{C}^{2\times2}, \quad \mathbf{b} \in \mathbb{C}^{1\times2}, \quad \xi \in \mathbb{C}, \quad \mathbf{0} = (0,0) \right\}. \tag{A1}$$

The set M is closed with respect to matrix multiplication and inverse operation, i.e., it forms a group,

$$M_1, M_2 \in \mathbb{M} \Rightarrow M_1 . M_2 \in \mathbb{M}, \quad M_a^{-1} \in \mathbb{M}, \quad a = 1, 2. \tag{A2}$$

Particularly, it is worth noticing that $S_1 \equiv \begin{pmatrix} 0 & 1 & 0 \\ 1 & 0 & 0 \\ 0 & 0 & 0 \end{pmatrix}$ belongs to $\mathbb{M}$. If we select the matrix U such that $U \in \mathbb{M}$,

then $U_x \in \mathbb{M}$, with $U_x \equiv \partial_x U$, leads to the relation

$$\delta V = i[S_1, U_x U^{-1}] = \begin{pmatrix} \mathbb{B} & \mathbf{b} \\ \mathbf{0} & 0 \end{pmatrix} \in \mathbb{M}, \qquad \text{(A3)}$$

which is manifestly non-Hermitian. The vector $\mathbf{b}$ can be nullified by a specific choice of the seed solutions. Nevertheless, the new potential δV becomes, again, block diagonal.

The latter reveals that to avoid non-Hermitian potential terms, we must work with at least two flat-band states

associated with the same flat-band level, rendering a transformation matrix with the structure

$$U = \begin{pmatrix} \mathbf{b} & \mathbb{B} \\ 0 & \boldsymbol{\xi} \end{pmatrix}, \quad \boldsymbol{\xi} = (\xi_1, \xi_2). \qquad \text{(A4)}$$

This ensures that the new Hamiltonians constructed using the supersymmetric transformation showcase all the desired properties.

---

[1] D. Leykam, A. Andreanov, and S. Flach, Artificial flat band systems: From lattice models to experiments, Adv. Phys. X **3**, 1473052 (2018).

[2] R. Drost *et al.*, Topological states in engineered atomic lattices, Nat. Phys. **13**, 668 (2017).

[3] M. R. Slot, S. N. Kempkes, E. J. Knol, W. M. J. van Weerdenburg, J. J. van den Broeke, D. Wegner, D. Vanmaekelbergh, A. A. Khajetoorians, C. Morais Smith, and I. Swart, p-band engineering in artificial electronic lattices, Phys. Rev. X **9**, 011009 (2019).

[4] L. Yan and P. Liljeroth, Engineered electronic states in atomically precise artificial lattices and graphene nanoribbons, Adv. Phys. X **4**, 1651672 (2019).

[5] S. E. Freeney *et al.*, Electronic quantum materials simulated with articial model lattices, ACS Nanosci. Au **2**, 198 (2022).

[6] R. A. Vicencio, C. Cantillano, L. Morales-Inostroza, B. Real, C. Mejia-Cortes, S. Weimann, A. Szameit, and M. I. Molina, Observation of localized states in Lieb photonic lattices, Phys. Rev. Lett. **114**, 245503 (2015).

[7] B. Real *et al.*, Flat-band light dynamics in Stub photonic lattices, Sci. Rep. **7**, 15085 (2017).

[8] T.-X. Ma *et al.*, Acoustic flat bands in phononic crystal defect lattices, J. Appl. Phys. **129**, 145104 (2021).

[9] P. Karki and J. Paulose, Nonsingular and singular flat bands in tunable phononic metamaterials, Phys. Rev. Res. **5**, 023036 (2023).

[10] M. N. Huda, S. Kezilebieke, and P. Liljeroth, Designer flat bands in quasi-one-dimensional atomic lattices, Phys. Rev. Res. **2**, 043426 (2020).

[11] E. Travkin, F. Diebel, and C. Denz, Compact flat band states in optically induced flatland photonic lattices, Appl. Phys. Lett. **111**, 011104 (2017).

[12] E. J. Meier, F. Alex An, and B. Gadway, Observation of the topological soliton state in the Su-Schrieffer-Heeger model, Nat. Commun. **7**, 13986 (2016).

[13] M. N. Huda, S. Kezilebieke, R. Drost, T. Ojanen, and P. Liljeroth, Tuneable topological domain wall states in engineered atomic chains, npj Quantum Mater. **5**, 17 (2020).

[14] J. Zurita, C. E. Creffield, and G. Platero, Topology and interactions in the photonic Creutz and Creutz-Hubbard Ladders, Adv. Quantum Technol. **3**, 1900105 (2020).

[15] D. Bercioux, O. Dutta, and E. Rico, Solitons in one-dimensional lattices with a flat band, Ann. Phys. (Berlin) **529**, 1600262 (2017).

[16] A. Anastasiadis, G. Styliaris, R. Chaunsali, G. Theocharis, and F. K. Diakonos, Bulk-edge correspondence in the trimer Su-Schrieffer-Heeger model, Phys. Rev. B **106**, 085109 (2022).

[17] S. Longhi, Aharonov-Bohm photonic cages in waveguide and coupled resonator lattices by synthetic magnetic fields, Opt. Lett. **39**, 5892 (2014).

[18] S. Mukherjee, M. Di Liberto, P. Öhberg, R. R. Thomson, and N. Goldman, Experimental observation of Aharonov-Bohm cages in photonic lattices, Phys. Rev. Lett. **121**, 075502 (2018).

[19] M. Kremer, I. Petrides, E. Meyer, M. Heinrich, O. Zilberberg, and A. Szameit, A square-root topological insulator with non-quantized indices realized with photonic Aharonov-Bohm cages, Nat. Commun. **11**, 907 (2020).

[20] A. Mukherjee, A. Nandy, S. Sil and A. Chakrabarti, Engineering topological phase transition and Aharonov-Bohm caging in a flux-staggered lattice, J. Phys.: Condens. Matter **33**, 035502 (2021).

[21] S. Shahbazi and M. V. Hosseini, Revival of superconductivity in a one-dimensional dimerized diamond lattice, Sci. Rep. **13**, 15725 (2023).

[22] M. Thumin and G. Bouzerar, Flat band superconductivity in a system with a tunable quantum metric: the stub lattice, Phys. Rev. B **107**, 214508 (2023).

[23] S. Mukherjee and R. Thomson, Observation of localized flat-band modes in a quasi-one-dimensional photonic rhombic lattice, Opt. Lett. **40**, 5443 (2015).

[24] S. Mukherjee and R. Thomson, Observation of robust flat-band localization in driven photonic rhombic lattices, Opt. Lett. **42**, 2243 (2017).

[25] F. Baboux *et al.*, Bosonic condensation and disorder-induced localization in a flat band, Phys. Rev. Lett. **116**, 066402 (2016).

[26] L. Morales-Inostroza and R. A. Vicencio, Simple method to construct flat-band lattices, Phys. Rev. A **94**, 043831 (2016).

[27] T. Mizoguchi and M. Udagawa, Flat-band engineering in tight-binding models: Beyond the nearest-neighbor hopping, Phys. Rev. B **99**, 235118 (2019).

[28] W. Maimaiti, A. Andreanov, H. C. Park, O. Gendelman, and S. Flach, Compact localized states and flat-band generators in one dimension, Phys. Rev. B **95**, 115135 (2017).

[29] C.-C. Lee, A. Fleurence, Y. Yamada-Takamura, and T. Ozaki, Hidden mechanism for embedding the flat bands of Lieb, kagome, and checkerboard lattices in other structures, Phys. Rev. B **100**, 045150 (2019).

[30] T. Ogata, M. Kawamura, and T. Ozaki, Methods for constructing parameter-dependent flat-band lattices, Phys. Rev. B **103**, 205119 (2021).

[31] F. Cooper, A. Khare, and U. Sukhatme, *Supersymmetry in Quantum Mechanics* (World Scientific, Singapore, 2001).

[32] L. M. Nieto, A. A. Pecheritsin, and B. F. Samsonov, Intertwining technique for the one-dimensional stationary Dirac equation, Ann. Phys. **305**, 151 (2003).

[33] E. Pozdeeva and A. Schulze-Halberg, Darboux transformations for a generalized Dirac equation in two dimensions, J. Math. Phys. **51**, 113501 (2010).

[34] S. Kuru, J. Negro, and L. M. Nieto, Exact analytic solutions for a Dirac electron moving in graphene under magnetic fields, J. Phys.: Condens. Matter **21**, 455305 (2009).

[35] B. Midya and D. J. Fernández, Dirac electron in graphene under supersymmetry generated magnetic fields, J. Phys. A: Math. Theor. **47**, 285302 (2014).

[36] A.-L. Phan, D.-N. Le, V.-H. Le, and P. Roy, Electronic spectrum of spherical fullerene molecules in the presence of generalized magnetic fields, Eur. Phys. J. Plus **135**, 6 (2020).

[37] M. Castillo-Celeita and D. J. Fernández, Dirac electron in graphene with magnetic fields arising from first-order intertwining operators, J. Phys. A: Math. Theor. **53**, 035302 (2020).

[38] D. J. Fernández, C. J. García, and D. O-Campa, Bilayer graphene in magnetic fields generated by supersymmetry, J. Phys. A: Math. Theor. **54**, 245302 (2021).

[39] A. Schulze-Halberg and P. Roy, Dirac systems with magnetic field and position-dependent mass: Darboux transformations and equivalence with generalized Dirac oscillators, Ann. Phys. **431**, 168534 (2021).

[40] M. Castillo-Celeita, A. Contreras-Astorga, and D. J. Fernández C., Complex supersymmetry in graphene, Eur. Phys. J. Plus **137**, 904 (2022).

[41] V. Jakubský and M. S. Plyushchay, Supersymmetric twisting of carbon nanotubes, Phys. Rev. D **85**, 045035 (2012).

[42] F. Correa and V. Jakubský, Confluent Crum-Darboux transformations in Dirac Hamiltonians with *PT*-symmetric Bragg gratings, Phys. Rev. A **95**, 033807 (2017).

[43] F. Correa and V. Jakubský, Twisted kinks, Dirac transparent systems and Darboux transformations, Phys. Rev. D **90**, 125003 (2014).

[44] A. Contreras-Astorga, F. Correa, and V. Jakubský, Super-Klein tunneling of Dirac fermions through electrostatic gratings in graphene, Phys. Rev. B **102**, 115429 (2020).

[45] V. Jakubský and K. Zelaya, Reflectionless pseudospin-1 Dirac systems via Darboux transformation and flat band solutions, Phys. Scr. **99**, 035220 (2024).

[46] W. P. Su, J. R. Schrieffer, and A. J. Heeger, Solitons in polyacetylene, Phys. Rev. Lett. **42**, 1698 (1979).

[47] A. J. Heeger, S. Kivelson, J. R. Schrieffer, and W.-P. Su, Solitons in conducting polymers, Rev. Mod. Phys. **60**, 781 (1988).

[48] J. K. Asbóth, L. Oroszlány, and A. Pályi, *A Short Course on Topological Insulators, Band Structure and Edge States in One and Two Dimensions* (Springer, Cham, 2016), Vol. 919.

[49] S.-G. Jeong and T.-H. Kim, Topological and trivial domain wall states in engineered atomic chains, npj Quantum Mater. **7**, 22 (2022).

[50] S.-G. Jeong, S.-H. Han, T.-H. Kim, and S. Cheon, Revealing inverted chirality of hidden domain wall states in multiband systems without topological transition, Commun. Phys. **6**, 262 (2023).

[51] G. Queraltó, M. Kremer, L. J. Maczewsky, M. Heinrich, J. Mompart, V. Ahufinger, and A. Szameit, Topological state engineering via supersymmetric transformations, Commun. Phys. **3**, 49 (2020).

[52] D. Viedma, G. Queraltó, J. Mompart, and V. Ahufinger, High-efficiency topological pumping with discrete supersymmetry transformations, Opt. Express **30**, 23531 (2022).

[53] Y. Betancur-Ocampo, and G. Monsivais, Identifying Klein tunneling signatures in bearded SSH lattices from bent flat bands, arXiv:2312.10621.

[54] S. Verma and T. K. Ghosh, Emergent SU(3) topological system in a trimer SSH model, arXiv:2401.11695.

[55] V. Jakubský and K. Zelaya, Landau levels and snake states of pseudo-spin-1 Dirac-like electrons in gapped Lieb lattices, J. Phys.: Condens. Matter **35**, 025302 (2023).

[56] V. Jakubský, Spectrally isomorphic Dirac systems: Graphene in an electromagnetic field, Phys. Rev. D **91**, 045039 (2015).

[57] M. Castillo-Celeita and V. Jakubský, Reduction scheme for coupled Dirac systems, J. Phys. A: Math. Theor. **54**, 455301 (2021).